Journal of Environmental Radioactivity 193–194 (2018) 44–56

Contents lists available at ScienceDirect

Journal of Environmental Radioactivity

journal homepage: www.elsevier.com/locate/jenvrad

Mapping radiation distribution on ground based on the measurement using an unmanned aerial vehicle

Shuangyue Zhang[a], Ruirui Liu[b,*], Tianyu Zhao[b]

[a] Department of Electrical and Systems Engineering, Washington University, St. Louis, MO, 63130, USA
[b] Department of Radiation Oncology, Washington University School of Medicine, St. Louis, MO, 63110, USA

ARTICLE INFO

Keywords:
Nuclear emergency monitoring
Radiological emergency monitoring
Decontamination monitoring
Radiation contamination mapping
Unmanned aerial vehicle
Reconstruction algorithm

ABSTRACT

Mapping the radiation distribution on ground during a radiological emergency monitoring, or decontamination mission is an important task. Accurate knowledge of the radioactivity distribution can help radiation workers locate the contamination, which reduces unnecessary radiation exposure to personnel and perhaps to some extent also the exposure to the public. Recently, radiation monitoring systems based on unmanned aerial vehicles (UAV) have been widely studied and employed. However, development of algorithms for mapping the contamination from measured data obtained by the detection system mounted on an UAV is still lacking. In this work, we implemented an advanced statistical reconstruction algorithm for mapping spread and point radiation contamination. The algorithm significantly improves accuracy in the scope and location of radiation contamination.

1. Introduction

Emergency monitoring plays a key role in responding to radiological and nuclear accidents. An effective emergency monitoring can help the first responders handle the situation properly and safely. In nuclear emergency monitoring, an important task is to characterize the radiation distribution on the contaminated ground in order to set up different response zones. For radiological emergencies, searching for radiological orphan sources could pose a complicated task that often demands speed and accuracy in hazardous or even life-threatening situations. Also for the regular nuclear decontamination task, determining the radiation contamination scope and location in a fast and accurate way deserves research attention. A detection system mounted in aerial vehicles, such as helicopters, have been deployed to tackle these difficulties. However, the crew operating the vehicle could be exposed to radiation (Pöllänen et al., 2009). As a result, a plethora of monitoring system have been developed based on unmanned aerial vehicles (UAV) (Becker and Farsoni, 2016; MacFarlane et al., 2014; Martin et al., 2016; Okuyama et al., 2005; Bogatov and Mazny, 2013). While most development has focused on detector development and integration with the UAV, very little has been done in developing radiation mapping algorithms for reconstruction radiation contamination distribution on the ground based on the measurement data taken by an UAV.

Previously, we proposed a methodology (Liu et al., 2015). The algorithm we developed leads to solving an ill-conditioned linear system, and the generalized minimal residual method (GMRES) combined with the Tikhonov regularization was used to solve the linear system. The previous algorithm performed well, however, there were weaknesses, for instance, multiple neighboring contamination locations could not be completely separated, and some artifacts existed on the boundaries of reconstructed region. This study is to provide solutions for problems unsolved in our previous work.

The radiation mapping algorithm discussed in this work could be potentially used in nuclear emergency monitoring, orphan source localization, and decontamination monitoring situations.

2. Materials and methods

2.1. Model for radiation mapping

The UAV follows the predefined square grids as shown in Fig. 1 during the course of data acquisition. The detector system mounted on the UAV takes readings in air point by point through the whole grid. A detailed description of the development of the reconstruction algorithm used for radiation distribution mapping based on aerial measurement data is given by Liu et al. (2015). In this study, we deal with the mapping algorithm. As displayed in Fig. 1, i and j are the indices used to describe grid G, and $G(i, j)$ is a specific point on the grid. During field monitoring, the UAV will move at a specific speed, allowing the

* Corresponding author.
E-mail address: liuruirui@wustl.edu (R. Liu).

https://doi.org/10.1016/j.jenvrad.2018.08.016
Received 24 May 2018; Received in revised form 22 August 2018; Accepted 23 August 2018

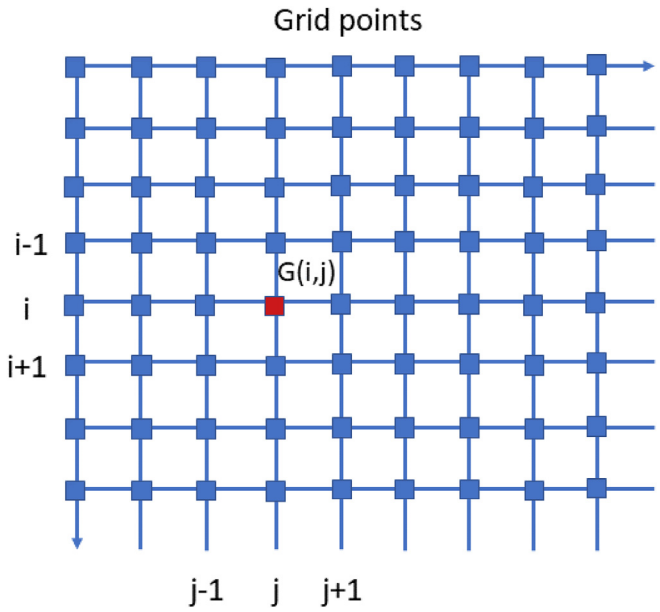

Fig. 1. Illustration of measurement grid distribution.

detector to measure just the grid point if the measurement time cycle has been set up appropriately. Note the following: $G(i,j)$ is the point at i-th row, j-th column on the grid; $\dot{N}(i,j)$is the count rate measured by the detector on the UAV at position; and $A(i,j)$is the radiation activity at position (i,j) on the ground.

The measured count rate at each grid point is contributed by radiation activity at all individual grid points, which is mathematically illustrated as

$$\begin{pmatrix} f_{1,1}^{1,1} & f_{1,2}^{1,1} & \cdots & f_{i,j}^{1,1} & \cdots & f_{n,n}^{1,1} \\ f_{1,1}^{1,2} & f_{1,2}^{1,2} & \cdots & f_{i,j}^{1,2} & \cdots & f_{n,n}^{1,2} \\ \vdots & \vdots & & \vdots & & \vdots \\ f_{1,1}^{i,j} & f_{1,2}^{i,j} & \cdots & f_{i,j}^{i,j} & \cdots & f_{n,n}^{i,j} \\ \vdots & \vdots & & \vdots & & \vdots \\ f_{1,1}^{n,n} & f_{1,2}^{n,n} & \cdots & f_{i,j}^{n,n} & \cdots & f_{n,n}^{n,n} \end{pmatrix} \begin{pmatrix} A_{11} \\ A_{12} \\ \vdots \\ A_{i,j} \\ \vdots \\ A_{nn} \end{pmatrix} = \begin{pmatrix} \dot{N}_{11} \\ \dot{N}_{12} \\ \vdots \\ \dot{N}_{i,j} \\ \vdots \\ \dot{N}_{nn} \end{pmatrix} \tag{1}$$

where $f_{i,j}^{I,J}$ is the detector response factor for grid position $G(i,j)$ when the detector is above the grid at $G(I,J)$, $A_{i,j}$ is the radiation activity at point $G(i,j)$, and $\dot{N}_{i,j}$ is the count rate measured in air above point $G(i,j)$. The linear system in equation (1) could be written in the matrix form as

$$\dot{N} = FA \tag{2}$$

where $\dot{N} = \begin{pmatrix} \dot{N}_{11} \\ \dot{N}_{12} \\ \vdots \\ \dot{N}_{ij} \\ \vdots \\ \dot{N}_{nn} \end{pmatrix}$, $A = \begin{pmatrix} A_{11} \\ A_{12} \\ \vdots \\ A_{ij} \\ \vdots \\ A_{nn} \end{pmatrix}$, and $F = \begin{pmatrix} f_{1,1}^{1,1} & f_{1,2}^{1,1} & \cdots & f_{i,j}^{1,1} & \cdots & f_{n,n}^{1,1} \\ f_{1,1}^{1,2} & f_{1,2}^{1,2} & \cdots & f_{i,j}^{1,2} & \cdots & f_{n,n}^{1,2} \\ \vdots & \vdots & & \vdots & & \vdots \\ f_{1,1}^{i,j} & f_{1,2}^{i,j} & \cdots & f_{i,j}^{i,j} & \cdots & f_{n,n}^{i,j} \\ \vdots & \vdots & & \vdots & & \vdots \\ f_{1,1}^{n,n} & f_{1,2}^{n,n} & \cdots & f_{i,j}^{n,n} & \cdots & f_{n,n}^{n,n} \end{pmatrix}$.

In equation (2), vector $\dot{N}$ could be obtained by measurements, while the response factor matrix, F, could be obtained by experimental measurements or analytical methods. An analytical method for calculating the response factor matrix was introduced by Liu et al. (2015). Here we simply introduce the calculation process. Mathematically, all elements of F are related by

$$f_{i,j}^{I,J} = f_{1,1}^{(1+|i-I|+|j-J|)} \tag{3}$$

where $f_{i,j}^{I,J}$ is the response factor for grid point $G(I,J)$ when the detector is above $G(I,J)$, and $f_{1,1}^{(1+|i-I|+|j-J|)}$ is the response factor for grid point $G(1+|i-I|+|j-J|)$ when the detector is above grid point $G(1,1)$. With the knowledge of the first column in F, the rest elements in F are calculated according to equation (3).

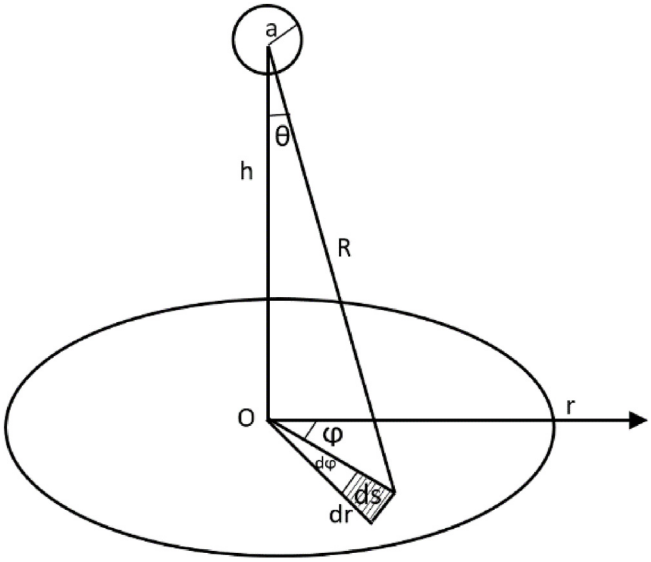

Fig. 2. Detection layout illustration.

As shown in Fig. 2, since the detector usually is high enough above the detecting infinitesimal area, ds on the ground, we can simplify that the detector is circular. The full detection solid angle is

$$\Omega(r) = 2\pi\left(1 - \frac{\sqrt{r^2+h^2}}{\sqrt{r^2+h^2+a^2}}\right) \tag{4}$$

where r is the lateral distance from detector, h is the detector height from ground, and a is the effective detector radius. With this, we define that is the full detection solid angle for the detector when it measures the radioactivity at grid point, $G(i,j)$, when above grid point $G(1,1)$. We define the response factor at grid point $G(i,j)$ with respect to grid point $G(1,1)$ as

$$f_{1,1}^{i,j} = \frac{\Omega_{1,1}^{i,j}}{4\pi}\eta \tag{5}$$

where η is the detection efficiency of the detector considering the air attenuation. The distance between grid $G(1,1)$ and grid $G(i,j)$ was found to be $r = \sqrt{(i-1)^2+(j-1)^2}L$. Based on equation (4), the detector response factor above grid $G(1,1)$ is given by

$$f_{1,1}^{i,j} = \frac{\eta}{2}\left(1 - \frac{\sqrt{(i-1)^2L^2+(j-1)^2L^2+h^2}}{\sqrt{(i-1)^2L^2+(j-1)^2L^2+h^2+a^2}}\right) \tag{6}$$

In responding to emergency monitoring, the activity vector can be solved by taking reading of count rate vector $\dot{N}$ in air through equation (2). From A the radiation activity on ground can be obtained. However, a straight-forward solution for equation (2) doesn't exist due to the ill-conditioned nature of the response factor matrix F. A statistical reconstruction algorithm is provided in this study as a quick and accurate solution for equation (2).

2.2. Reconstruction algorithm for radiation mapping

Our solution for the highly ill-conditioned inverse problem is regularized statistical image reconstruction (SIR) method. The linear system in a general form is

$$F\mathbf{x} = \mathbf{b}, \tag{7}$$

where $\mathbf{x} = [x_1 \ x_2 \ \cdots \ x_n]^T$, $\mathbf{b} = [b_1 \ b_2 \ \cdots \ b_m]^T$, and $F = [f_{i,j}]_{m\times n}$. In the radiation mapping described above, bis the measurement of $\dot{N}$ and